Supporting Information

Modification of Nickel Surfaces by Bismuth: Effect on Electrochemical Activity and Selectivity Towards Glycerol

Mohamed S. E. Houache[†], Kara Hughes[†], Reza Safari[‡], Gianluigi A. Botton[‡], Elena A. Baranova[†]*

[†]Department of Chemical and Biological Engineering, Centre for Catalysis Research and Innovation (CCRI), University of Ottawa, 161 Louis-Pasteur Ottawa ON, Canada, K1N 6N5.
[‡]Department of Materials Science and Engineering, McMaster University, 1280 Main St. W. Hamilton, ON, Canada, L9H 4L7.

*Corresponding author: Tel: 16135625800 (x 6302); fax: 16135625172;

E-mail: elena.baranova@uottawa.ca (Elena A. Baranova)

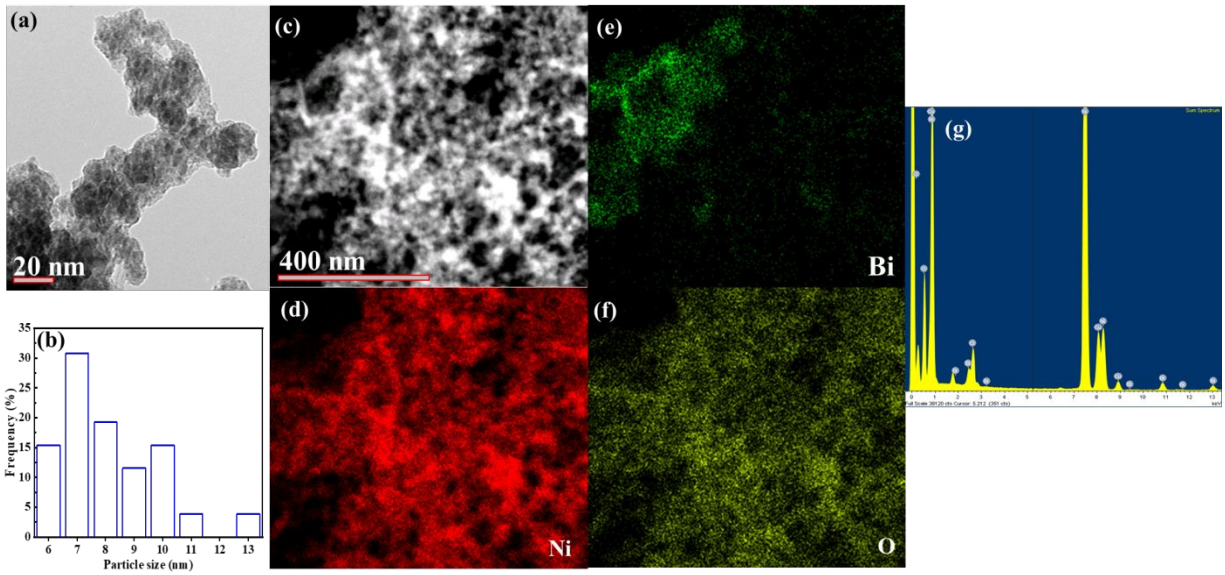

Figure S1. (a) STEM bright-field image of $Ni_{98}Bi_2$ nanoparticles, (b) Particle size distribution histograms, (c) HAADF-STEM image, (d-f) STEM-EDS mapping images for Ni, Bi and O elements, respectively and (g) EDS spectrum of $Ni_{98}Bi_2$.

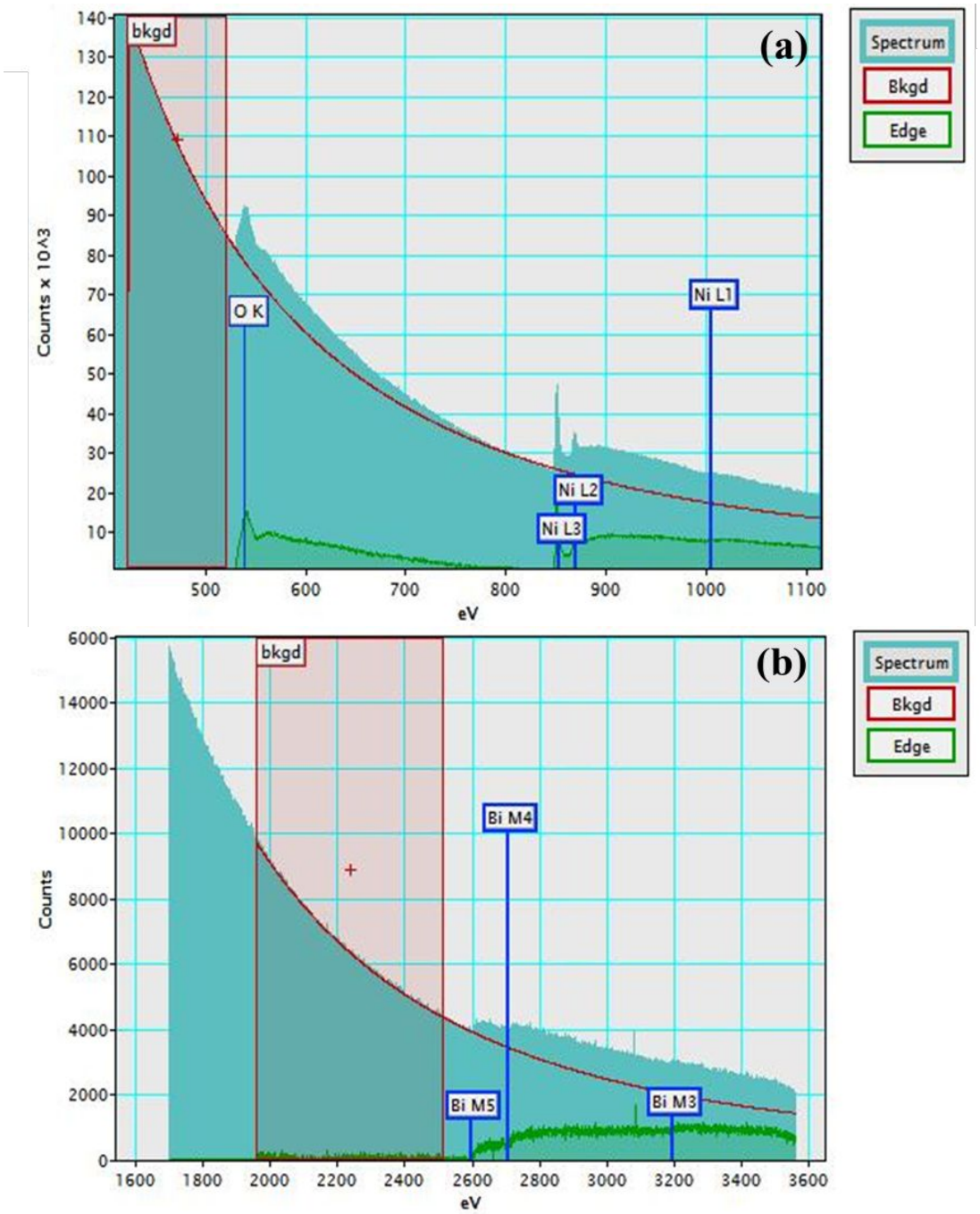

Figure S2. $Ni_{90}Bi_{10}$ EELS Spectrum Obtained at High Spatial Resolution of a) O-K and Ni-$L_{3,2}L_1$ and b) Bi-$M_{5,4}M_3$.

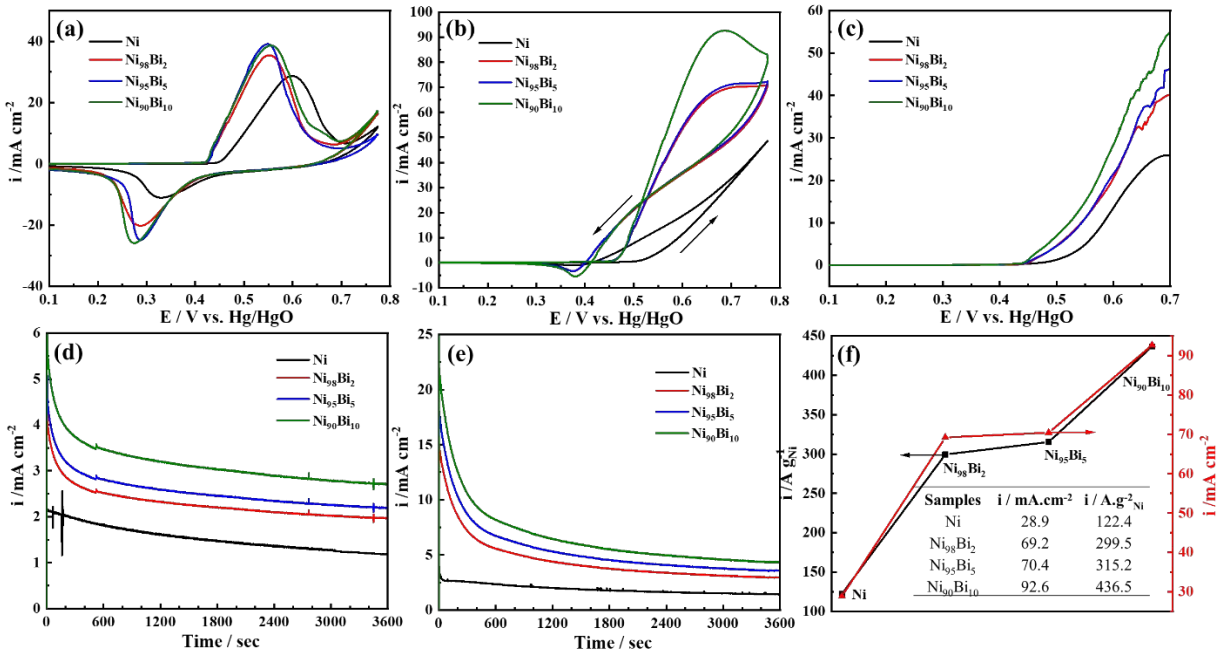

Figure S3. Cyclic voltammograms of Ni-based catalysts Ni_xBi_{1-x} performed in (a) 1 M KOH solution and (b) 1M KOH + 0.1M glycerol solution at scan rate of 50 mV s^{-1}. (c) Linear sweep voltammetry (LSV) at 1 mV s^{-1}. (d-e) CA tests at potential of 0.48 and 0.52 V vs. Hg/HgO for 60 min. (f) Comparison of current density after normalization to the Ni mass and the geometric surface area of the GC (0.196 cm^2).

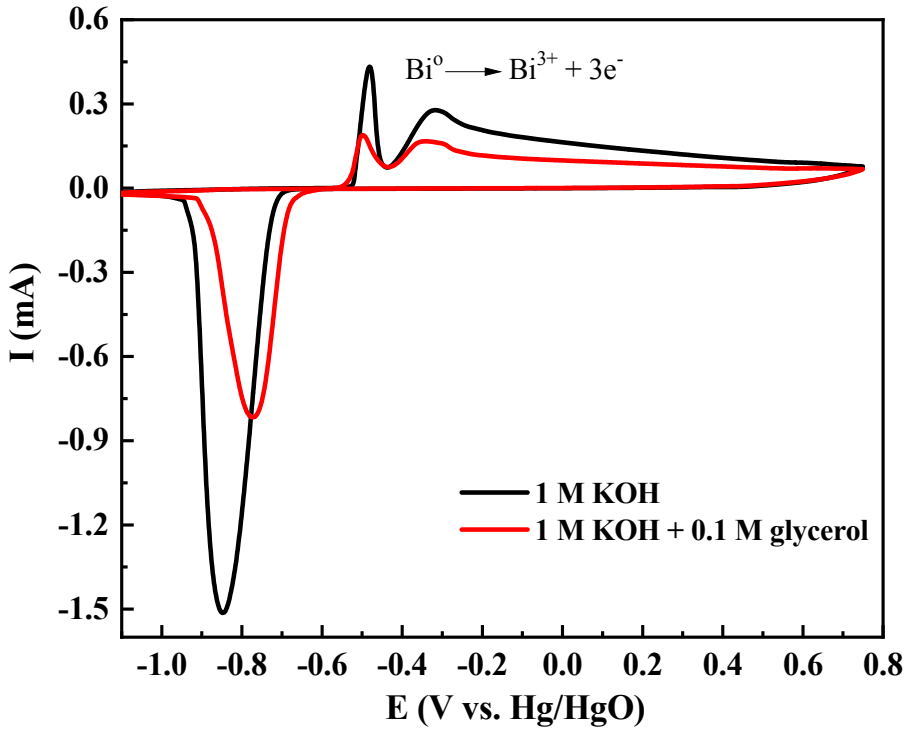

Figure S4. Cyclic voltammograms of Bi catalyst in 1 M KOH (black line) and 1M KOH + 0.1M glycerol (red line) at scan rate of 50 mV sec^{-1}.

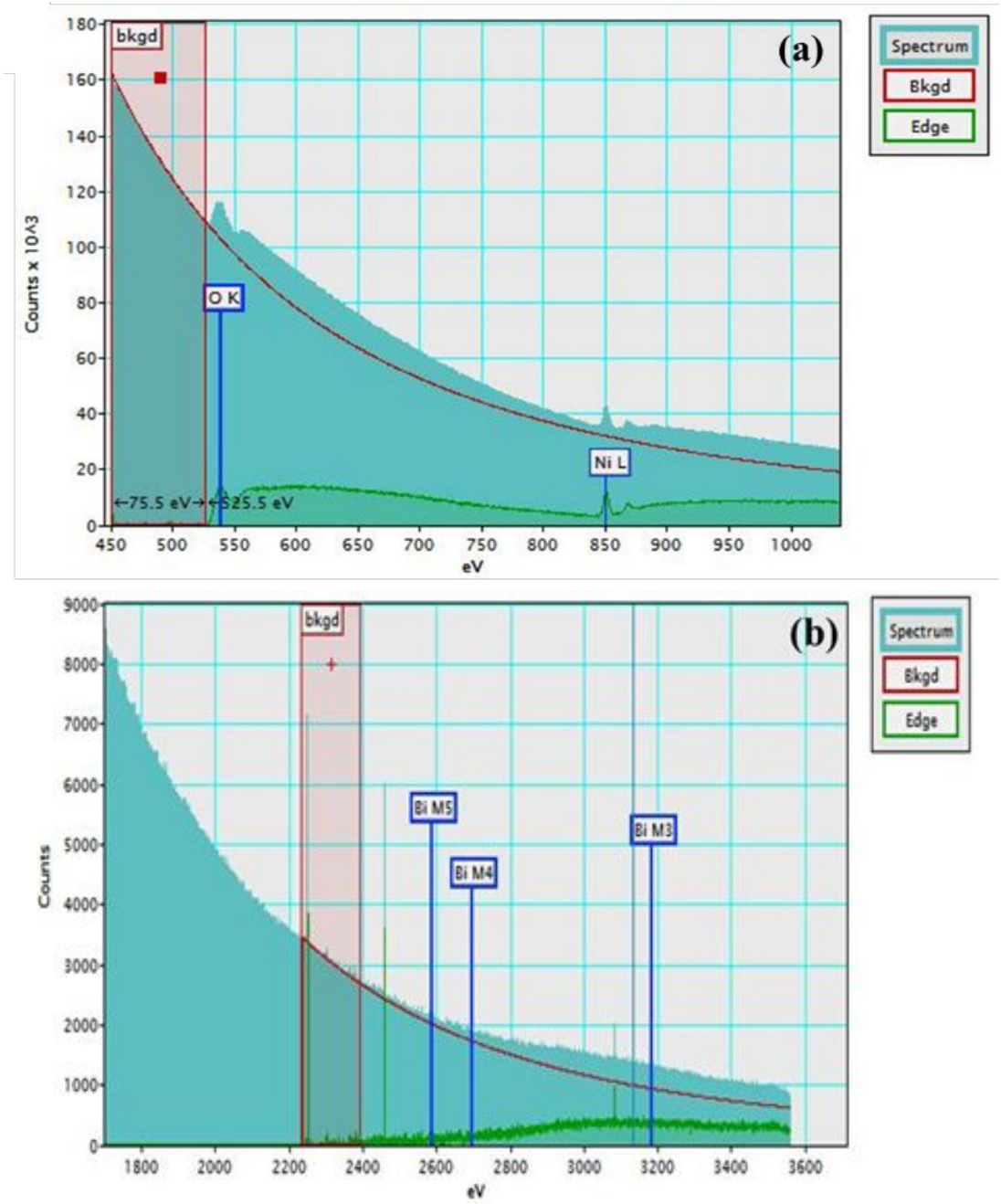

Figure S5. $Ni_{90}Bi_{10}$ after aging EELS spectrum obtained at high spatial resolution of a) O-K and Ni-$L_{3,2}L_1$ edges and b) Bi-$M_{5,4}M_3$ edges.

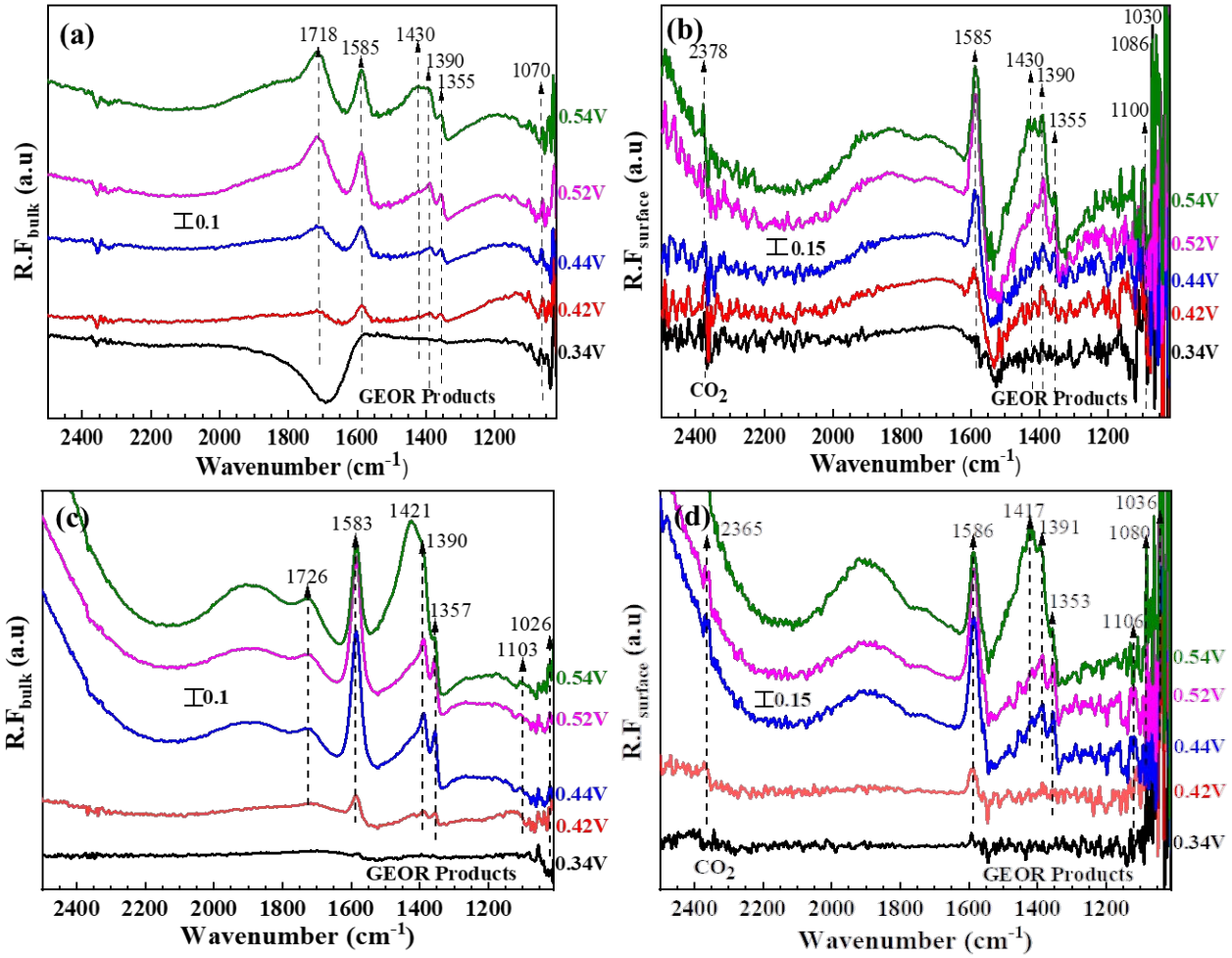

Figure S6. PM-IRRAS spectra during glycerol electro-oxidation on (a,b) $Ni_{95}Bi_5$ and (c,d) $Ni_{95}Bi_{5\text{-}aging\text{-}2w}$ in 1M KOH+0.1 M glycerol at various potentials as indicated in the figure. The left-hand spectra illustrate oxidation species in the thin cavity/bulk solution, while the right-hand spectra illustrate oxidation species on the surface.

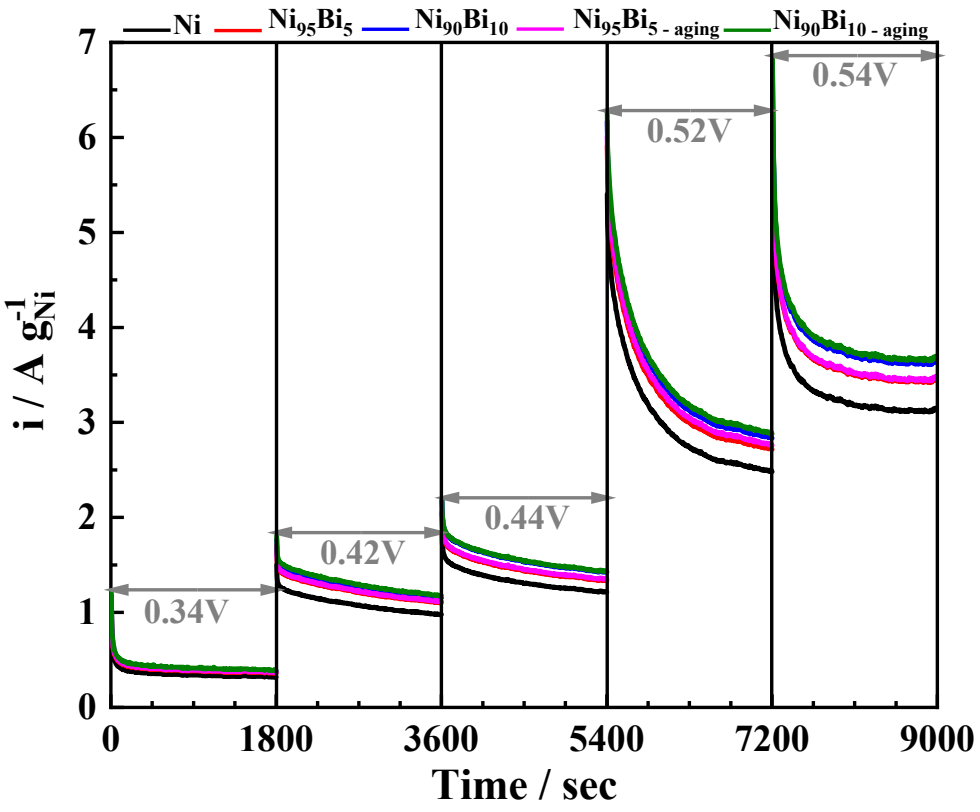

Figure S7. CA profile in 1M KOH+0.1M glycerol at different potentials, as specified by the double arrows for PM-IRRAS spectra.

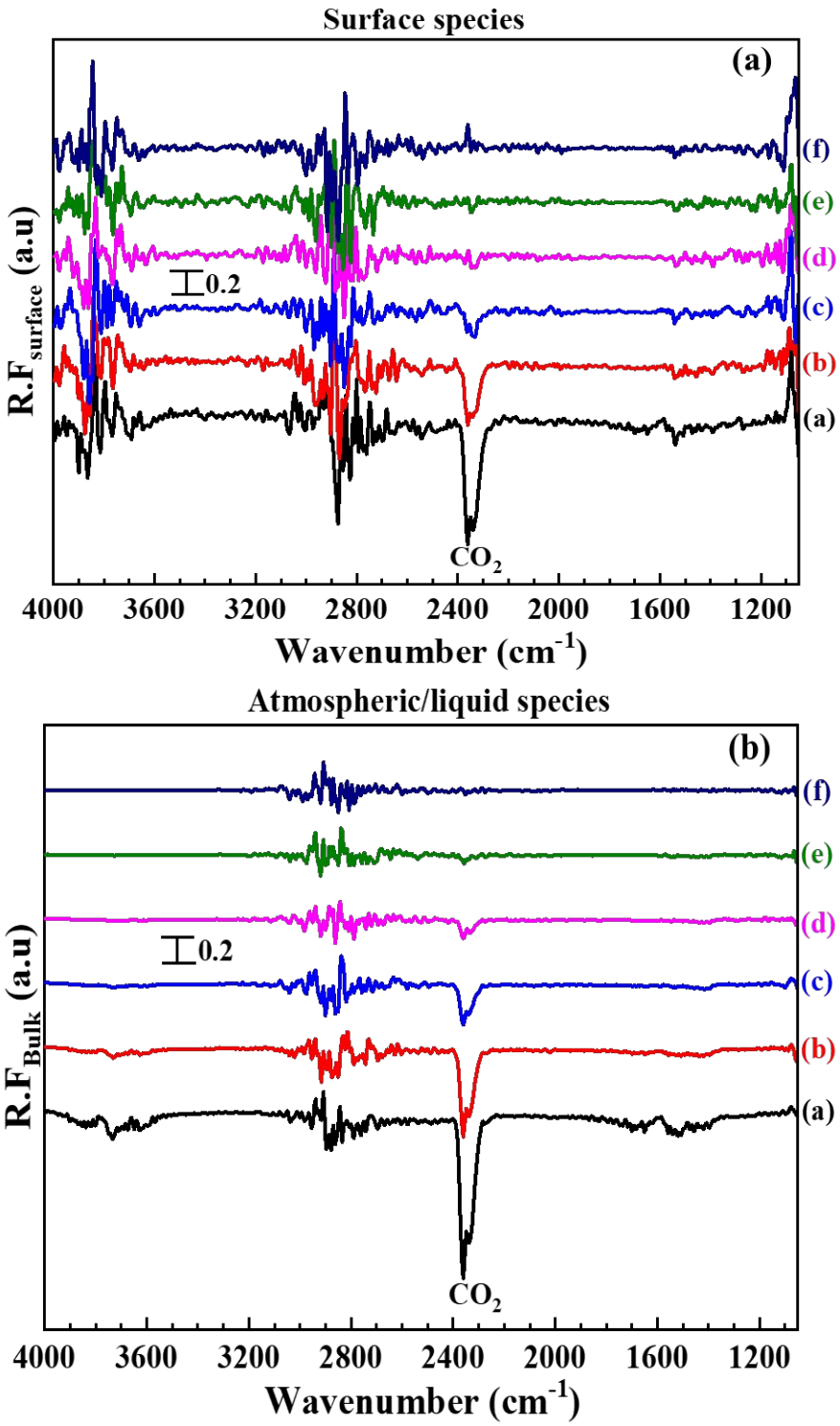

Figure S8. CO_2 tracking level background PM-IRRAS spectra of Ni-based catalyst in 1M KOH+0.1 M glycerol at open circuit potential (OCP); (a) 2.5 hrs., (b) 2 hrs., (c) 1.5 hrs., (d) 1 hr., (e) 30 min, and (f) 3min before measurements were initiated

Table S1. Assignment of the main bands in the spectra of the figure 7 (a-f) and SI. 4 (a-d)

Wavenumber (cm^{-1})					Assignment
Ni	**$Ni_{95}Bi_5$**	**$Ni_{90}Bi_{10}$**	**$Ni_{95}Bi_{5\ aging}$**	**$Ni_{90}Bi_{10\ aging}$**	
$1035^{b,s}$	$1030^{b,s}$	1028^{s} / 1030^{b}	1026^{b} / 1036^{s}	1028^{b} / 1035^{s}	ν (C-O) of alcohols
1085^{s}	1070^{s} / 1086^{b}	1063^{s}	1080^{s}	$1062^{b,s}$	ν (C-O) of alcohols
1112^{s}	1100^{s}	1102^{b} / 1118^{s}	1103^{b} / 1106^{s}	$1100^{b,s}$	ν (C-O) of alcohols
		1219^{s}			ν (C-O) of carboxylic acids, ν (C-O) of aliphatic ketones, δ(OH) of alcohols
$1358^{b,s}$	$1355^{b,s}$	$1345^{b,s}$	1353^{s} /1357^{b}	1355^{s} /1357^{b}	ν $(O\text{-}C\text{-}O)_s$ of carboxylates; ν (C-C) of aliphatic ketones, δ(OH) of alcohols
$1385^{b,s}$	$1390^{b,s}$	$1388^{b,s}$	$1390^{b,s}$	1386^{b} /1390^{s}	ν $(O\text{-}C\text{-}O)_s$ of carboxylates and carbonate; $\delta(CH_3)_s$ of methyl groups; δ(OH) of alcohols
$1422^{b,s}$	$1430^{b,s}$		1417^{s} / 1421^{b}	1417^{b} / 1438^{s}	ν $(O\text{-}C\text{-}O)_s$ of carboxylates and carbonate; δ(OH) of alcohols
				1506^{s}	$\delta(CH_2)$ scissor vibration
$1583^{b,s}$	$1585^{b,s}$	$1584^{b,s}$	1583^{b} / 1586^{s}	1581^{s}/ 1589^{b}	ν $(O\text{-}C\text{-}O)_{as}$ of carboxylates; ν (C≡C) of enols
	1718^{b}	1723^{b}	1726^{b}	1710^{b}	ν (C=O) carboxylic acids, aldehydes and ketones
2356^{s}	2378^{s}	2341^{s} / 2357^{b}	2365^{s}	2362^{s}	ν $(O{=}C{=}O)_{as}$

Subscripts indicate the type of oxidation species: b – in thin cavity/bulk solution, s – on the surface.

Notation used for mode description: ν – stretching; δ – deformation.

Subscripts illustrate the type of mode: s – symmetric, as – asymmetric.

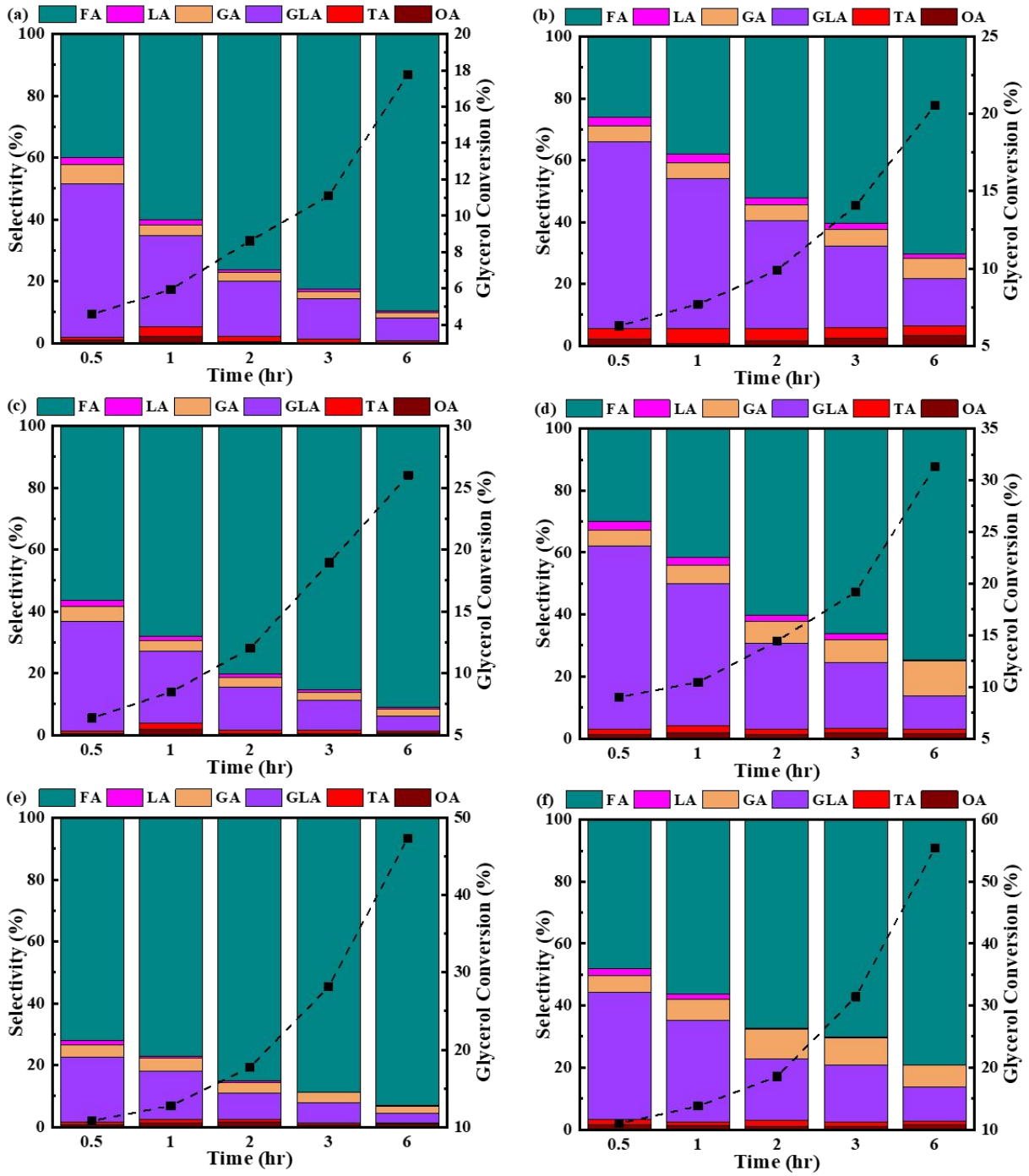

Figure S9. Product distributions and glycerol conversion (dashed line) on Ni at different applied potentials for different reaction time (a,b) 1.3 V, (c,d) 1.4 V and (e,f) 1.55 V, in a 1M KOH+0.1 M glycerol. The left-hand figures illustrate product distributions at room temperature, while the right-hand illustrates products at 50 ^{0}C. Green: formate; Pink: lactate; Orange: glycolate; Violet: glycerate; Red: tartronate and Brown: oxalate.

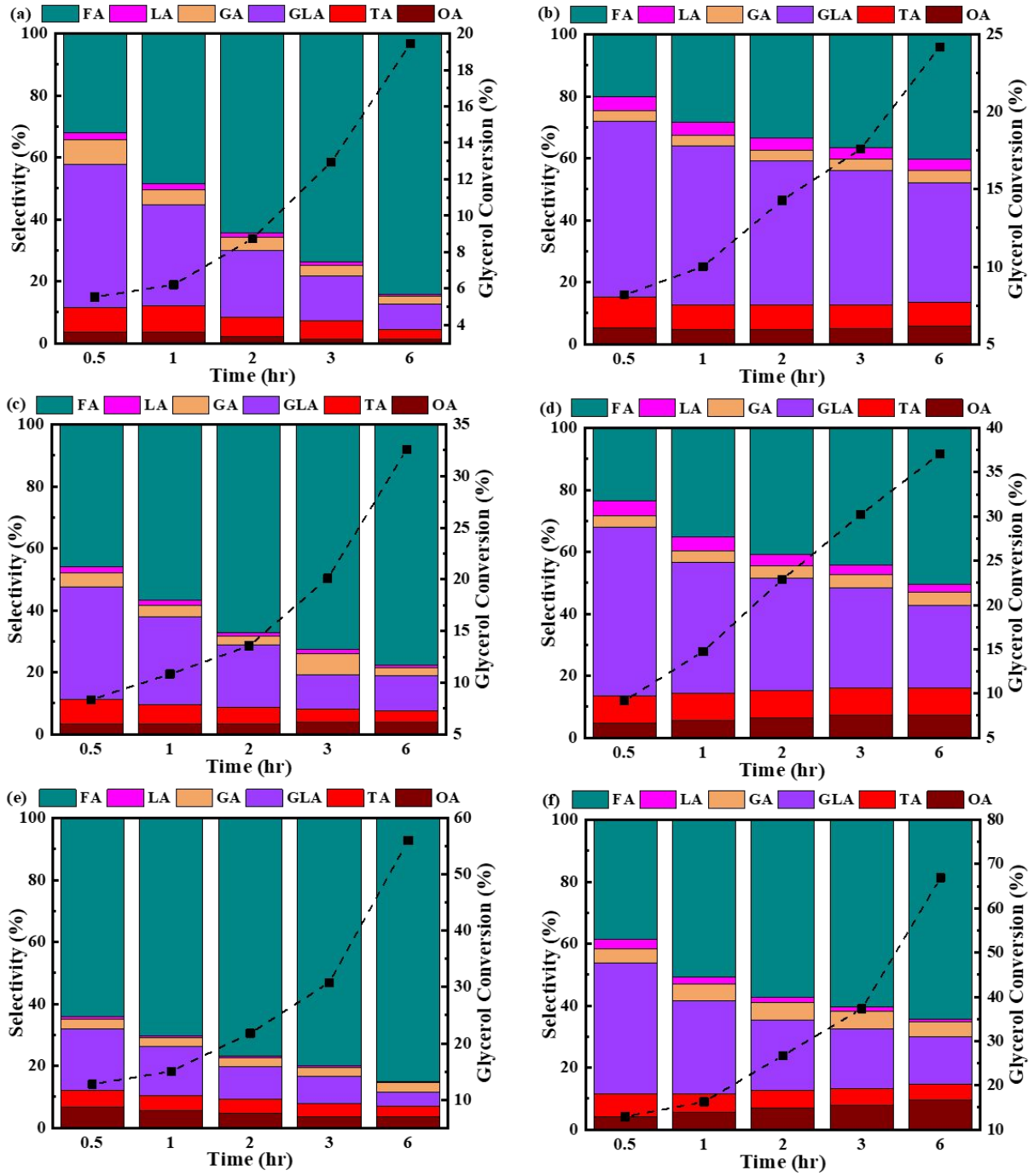

Figure S10. Product distributions and glycerol conversion (dashed line) on $Ni_{90}Bi_{10}$ at different applied potentials for different reaction time (a,b) 1.3 V, (c,d) 1.4 V and (e,f) 1.55 V, in a 1M KOH+0.1 M glycerol. The left-hand figures illustrate product distributions at room temperature, while the right-hand illustrates products at 50 ^{0}C. Green: formate; Pink: lactate; Orange: glycolate; Violet: glycerate; Red: tartronate and Brown: oxalate.

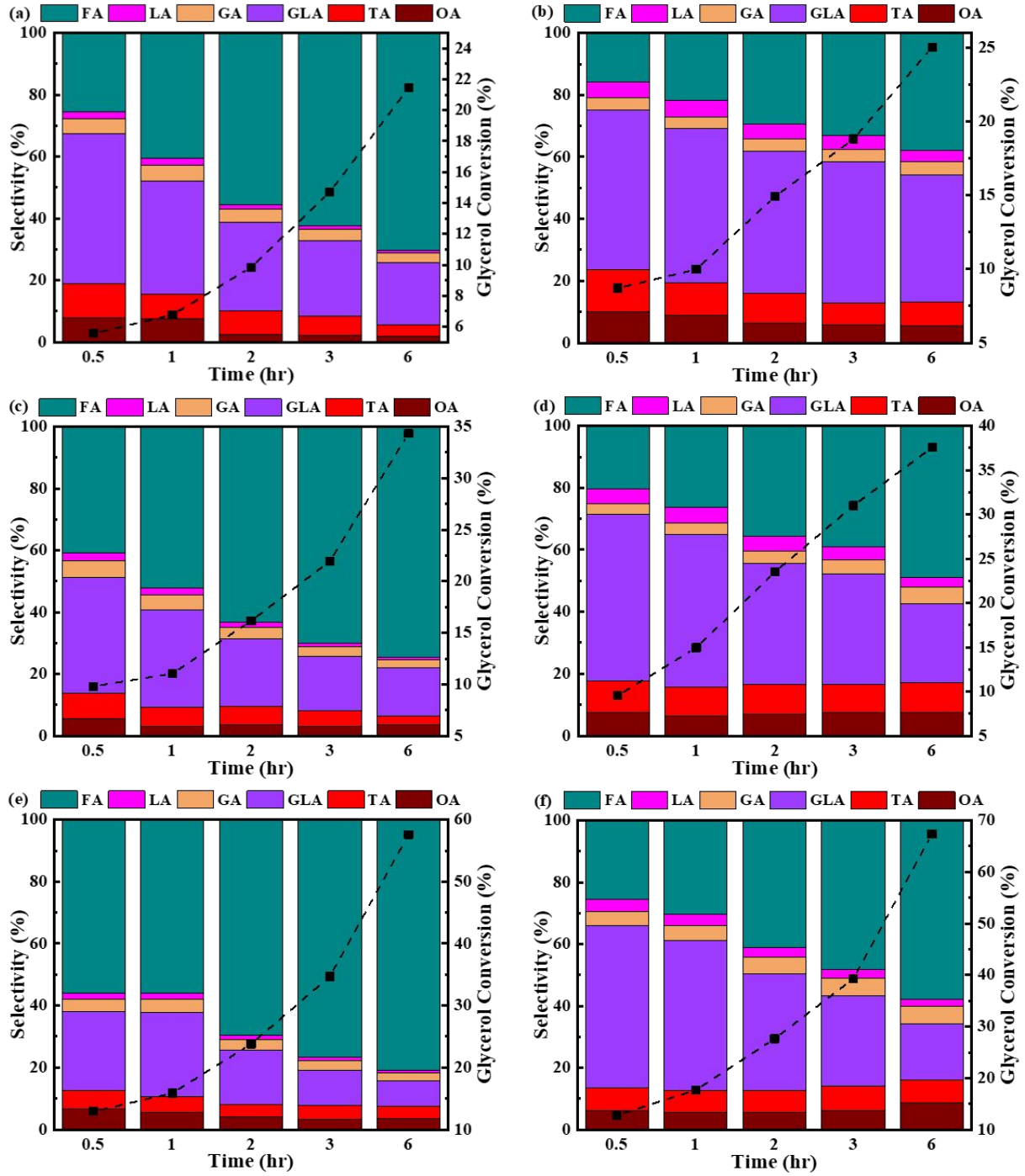

Figure S11. Product distributions and glycerol conversion (dashed line) on $Ni_{90}Bi_{10\text{-aging-2w}}$ at different applied potentials for different reaction time (a,b) 1.3 V, (c,d) 1.4 V and (e,f) 1.55 V, in a 1M KOH+0.1 M glycerol. The left-hand figures illustrate product distributions at room temperature, while the right-hand illustrates products at 50 ^{0}C. Green: formate; Pink: lactate; Orange: glycolate; Violet: glycerate; Red: tartronate and Brown: oxalate.

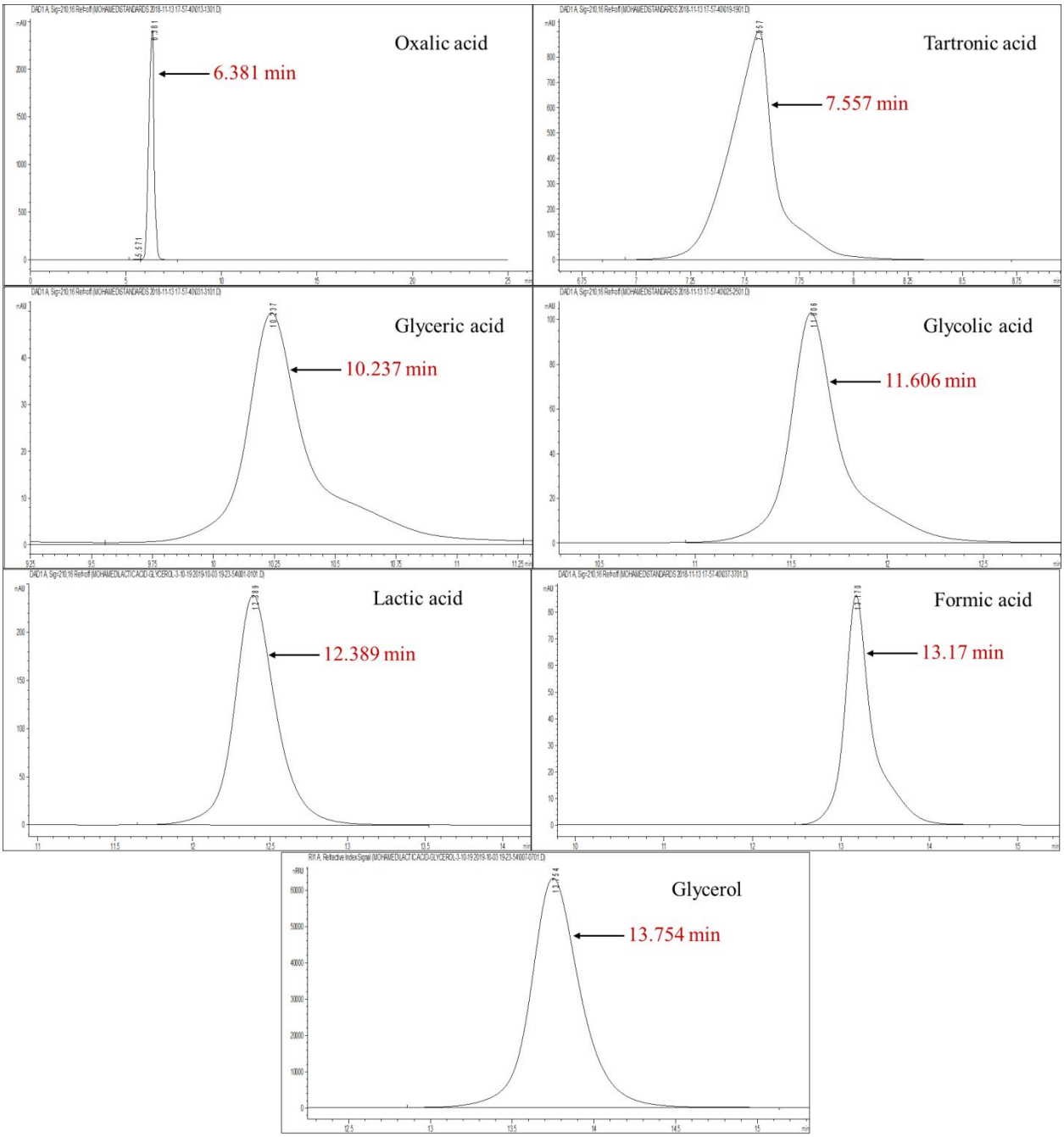

Figure S12. Chromatograms of the standards using DAD (diode array detector) UV/Vis detector at 210 nm for GEOR products and refractive index signal for glycerol. Each sample consist of 1 M KOH with 0.12M of the chosen analyte.

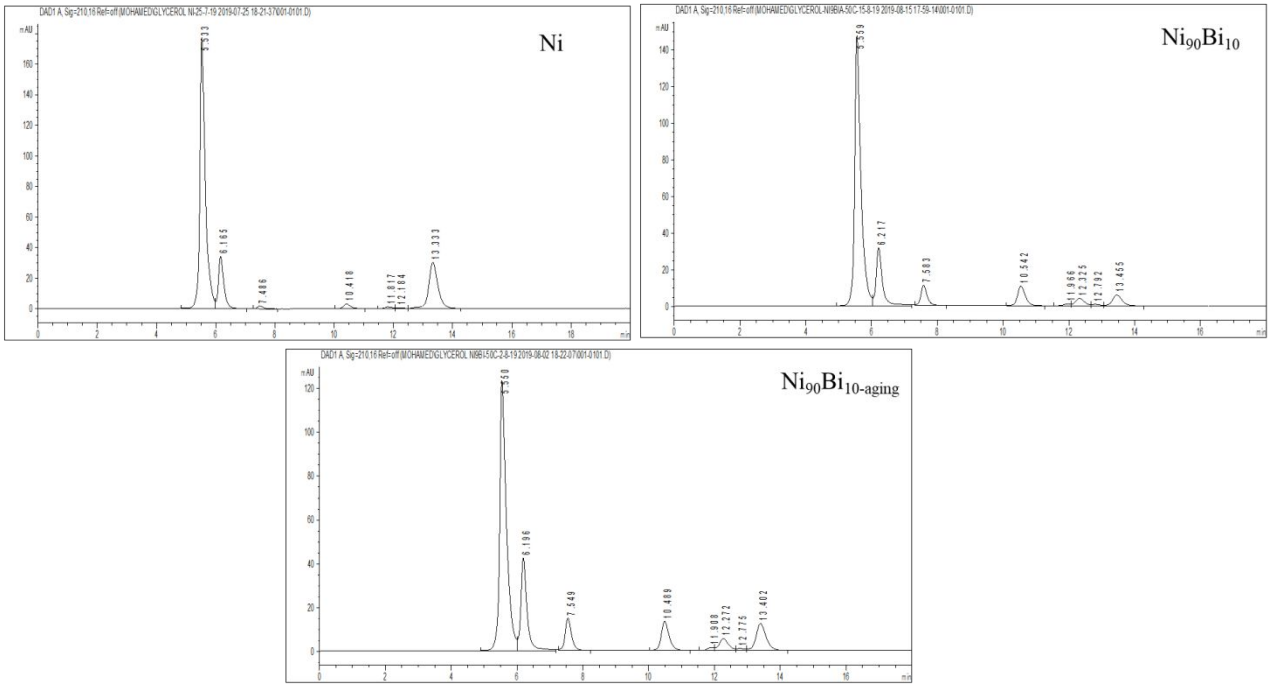

Figure S13. Chromatograms of the samples using DAD (diode array detector) UV/Vis detector at 210 nm for GEOR products at 1.3 V in a 1M KOH + 0.1 M glycerol after 30 min electrolysis.

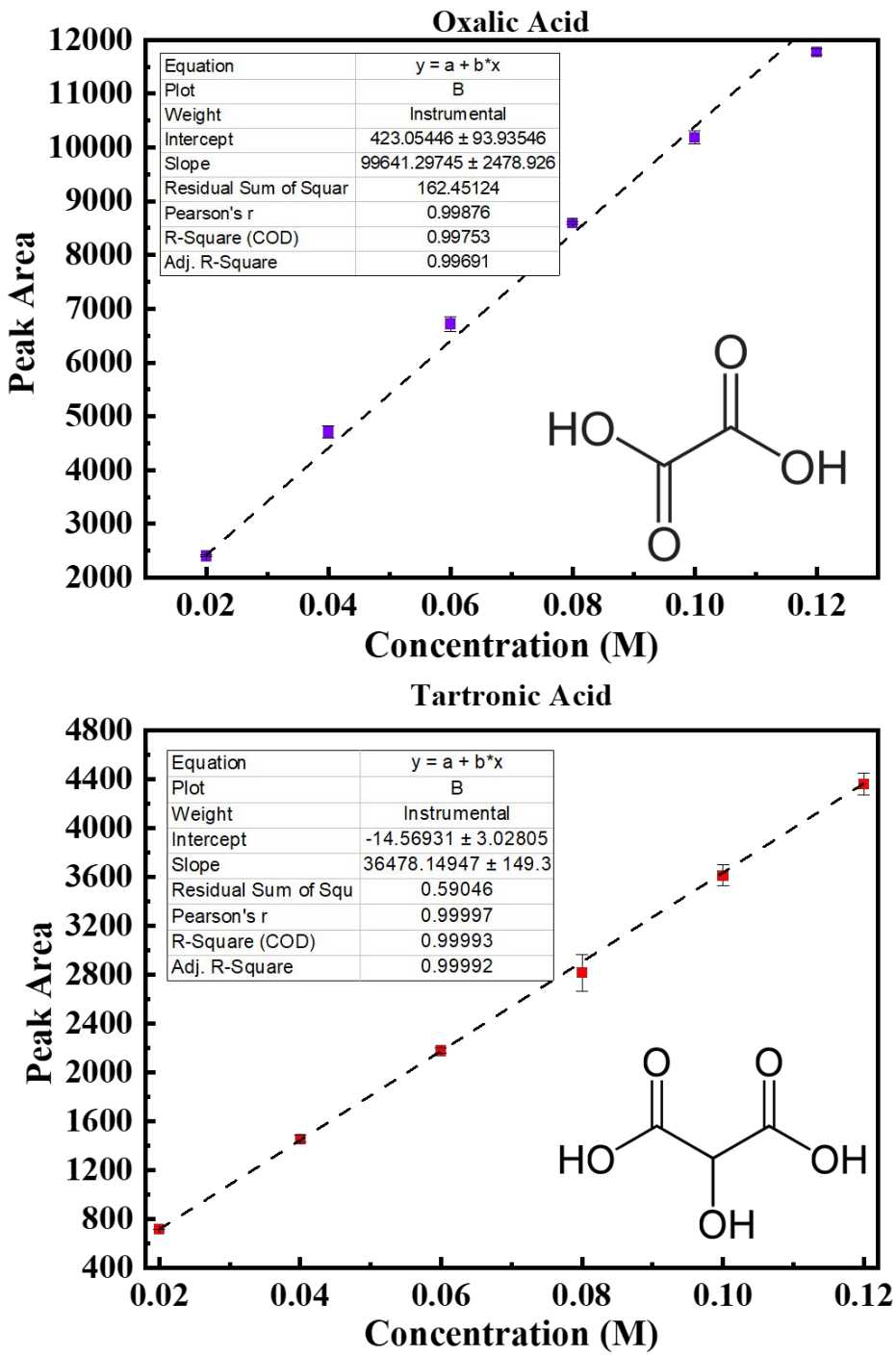

Figure S14. Calibrated curves of oxalic and tartronic acids determined from HPLC with retention time of 6.23 and 7.58 min, respectively using DAD (diode array detector) UV/Vis detector 210 nm.

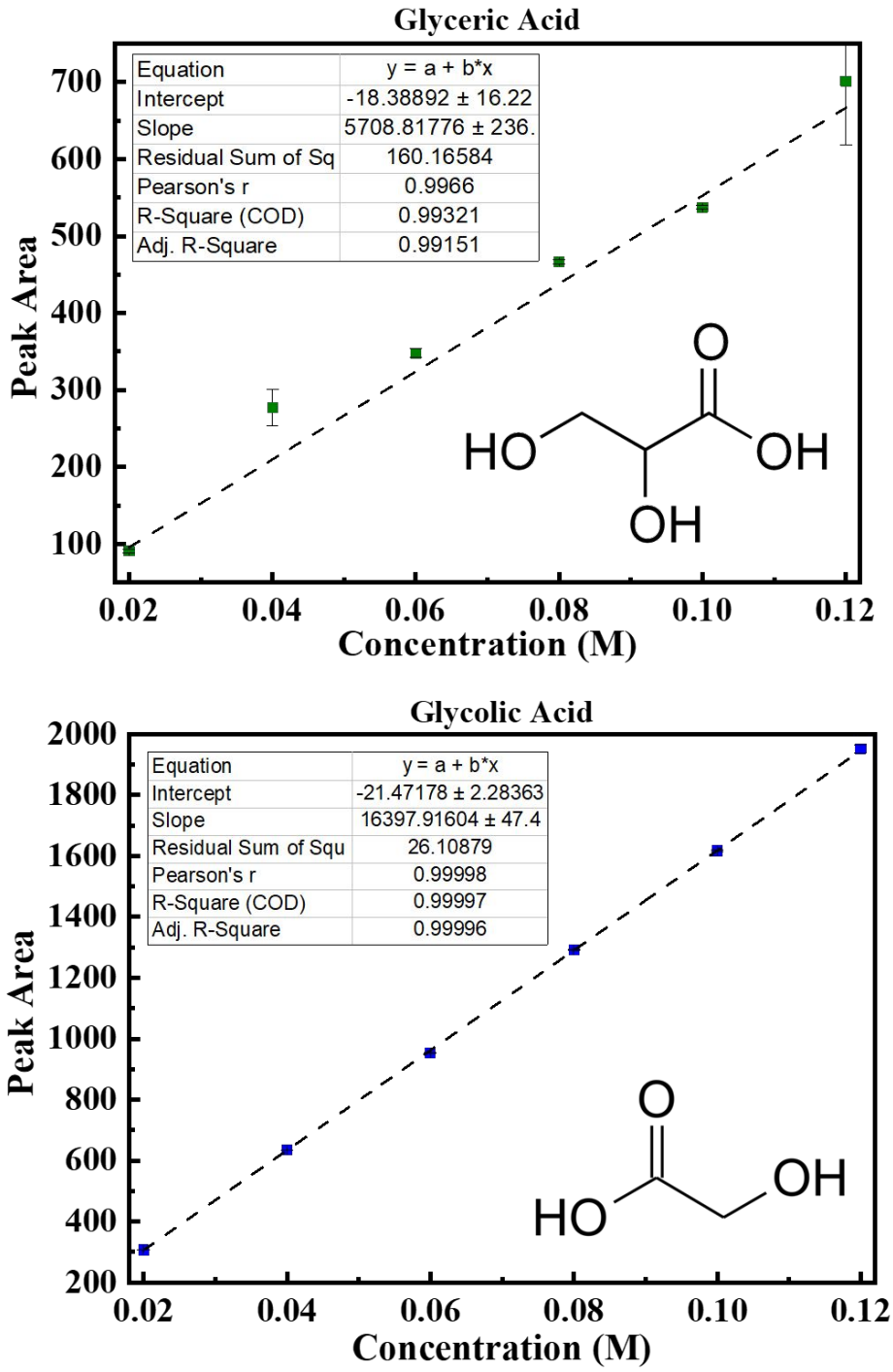

Figure S15. Calibrated curves of glyceric and glycolic acids determined from HPLC with retention time of 10.41 and 11.81 min, respectively using DAD (diode array detector) UV/Vis detector 210 nm.

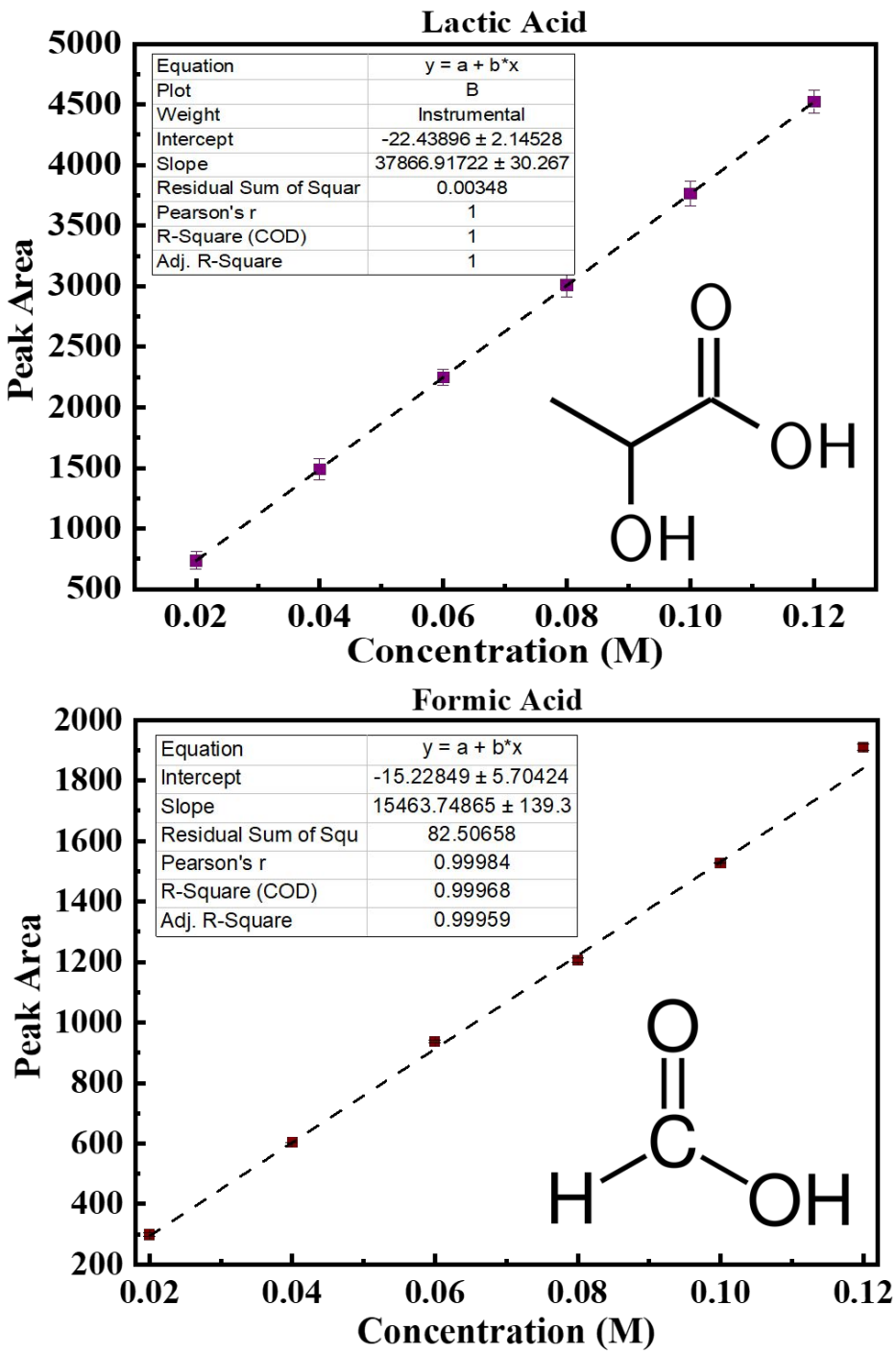

Figure S16. Calibrated curves of lactic and formic acids determined from HPLC with retention time of 12.39 and 13.47 min, respectively using DAD (diode array detector) UV/Vis detector 210 nm.

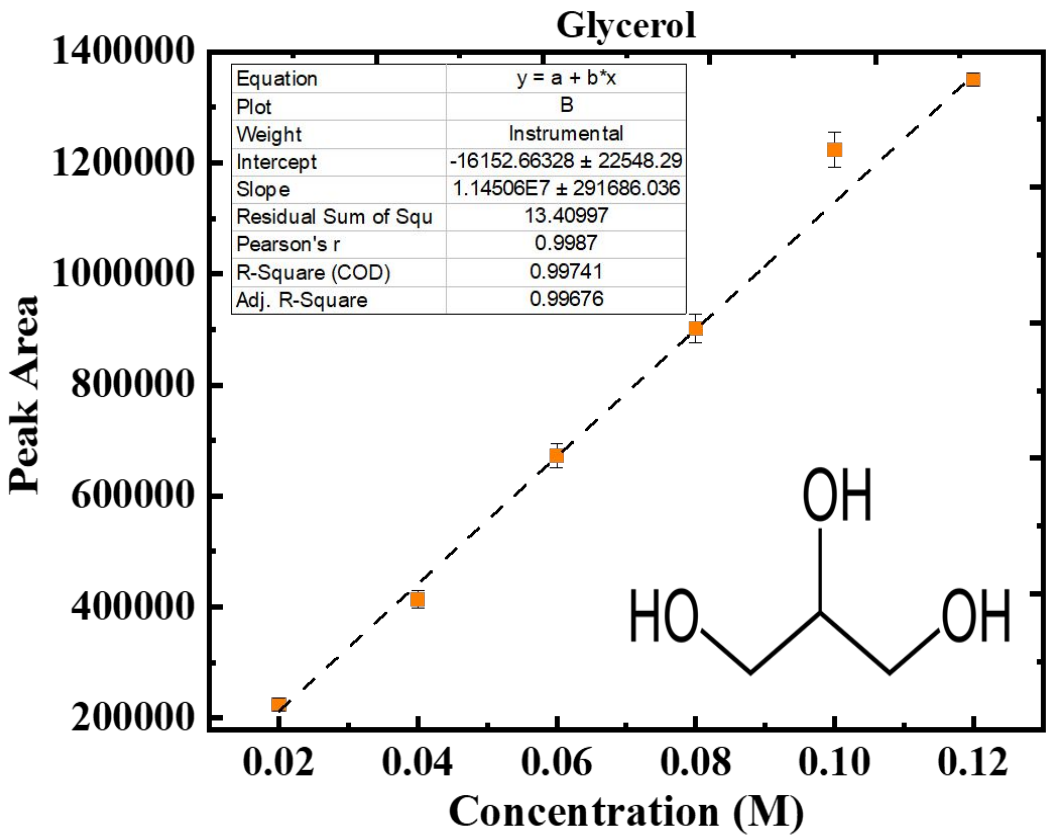

Figure S17. Calibrated curves of glycerol determined from HPLC with retention time of 13.74 using refractive index signal.

Table S2. Comparison of performance reported in the open literature for PGM free catalysts.

Catalyst	Synthesis	Electrolyte	E_{onset} vs. RHE (V)	Conditions	Selectivity	Ref.
Spherical Ni	Heatless $NaBH_4$ reduction	0.1 M glycerol + 1 M KOH	1.375	CA –1.4 V; 30 min	OX: 0.6%, TA: 0.85% GA: 4.75%, GLYC:35.3%, LA:2%, FA:56.5% [h]	This work
$Ni_{90}Bi_{10}$			1.33		OX: 3.3%, TA: 7.9% GA: 4.5%, GLYC:36.3%, LA:2.1%, FA:45.8% [h]	
$Ni_{90}Bi_{10\text{-after aging}}$			1.33		OX: 5.5%, TA: 8.2% GA: 5.4%, GLYC:37.5%, LA:2.5%, FA:40.9% [h]	
Ni/C	Commercial	0.1 M glycerol + 0.1 M KOH	1.43	CA – 0.7 V vs. Hg/HgO; 3 h	DHA: 1.5% GLYD: 3.1%, GLYC: 29.8%, HPA: 17.9%, GA: 28.2%, OX: 4.1% [h]	1
ALD (TiO_2)-Ni/C	Commercial/TiO_2 deposition		1.39		DHA: 4%, GLYD: 0.9%, HPA: 10.1%, TA, 3.7%, GLYC: 24%, OX: 4.8%, FA: 1.4% [h]	
Bulk Ni	Commercial	0.1 M glycerol + 1 M KOH	1.37	CA – 0.42 to 0.54 V vs. Hg/HgO; 30 min	GLYD, carbonyl species, carboxylates [p]	2
Bulk $Ni_{\text{after treatment}}$			1.33			
Co_3O_4/GPE	Electrodeposition / annealing in air	0.5 M glycerol +1 M KOH	1.3	CA– 0.6 V vs. Hg/HgO; 24 h	FA [n]	3
Urchin Ni	Modified Polyol Method	0.5 M glycerol + 1 M KOH	1.3	CA – 0.42 to 0.54 V vs. Hg/HgO; 30 min	GLYD, carbonyl species, carboxylates [p]	4
$Ni_{80}Pd_{20}$			1.21			
Ni/C	Impregnation/ Reduction method	0.1 M glycerol + 0.1 M NaOH	1.3	CA – 1.6 V vs. RHE; 8 h	FA: 32.2%, GA: 11.5%, GLYC: 0.5 mM [h]	5
NiCo/C			1.44		FA: 7.5%, GA: 4.5%, GLYC: 0.25 mM [h]	
NiFe/C			1.2		FA: 4%, GA: 3.7%, GLYC: 0.1 mM [h]	
NiFeCO/C			1.25		FA: 34.1%, GA: 10.3%, GLYC: 0.2 mM [h]	
Bulk Ag	Commercial	1 M glycerol + 0.1 M NaOH	0.8	CA – 1.125 V vs. RHE; 14 h	FA, GA, GLYC [h]	6

Abbreviations: tartronic acid (TA), dihydroxyacetone (DHA), glyceraldehyde (GLYD), glyceric acid (GLYC) and hydroxypyruvic acid (HPA), glycolic acid (GA), oxalic acid (OX), lactic acid (LA) and formic acid (FA)
Subscripts illustrate the type of detection technique: (h) HPLC, (n) NMR and (p) PM-IRRAS

References

(1) Han, J.; Kim, Y.; Kim, H.W.; Jackson, D.H.; Lee, D.; Chang, H.; Chae, H.J. Lee, K.Y.; Kim, H.J. Effect of Atomic Layer Deposited TiO_2 on Carbon-Supported Ni Catalysts for Electrocatalytic Glycerol Oxidation in Alkaline Media. *Electrochem. Commun.*, **2017**, *83*, 46-50.
(2) Houache, M. S. E.; Cossar, E.; Ntais, S.; Baranova, E. A. Electrochemical Modification of Nickel Surfaces for Efficient Glycerol Electrooxidation. *J. Power Sources*, **2018**, *375*, 310-319.
(3) Sun, S.; Sun, L.; Xi, S.; Du, Y.; Prathap, M.A.; Wang, Z.; Zhang, Q.; Fisher, A.; Xu, Z.J. Electrochemical Oxidation of C3 Saturated Alcohols on Co_3O_4 in Alkaline. *Electrochim. Acta*, **2017**, *228*, 183-194.
(4) Houache, M. S. E.; Hughes, K.; Ahmed, A.; Safari, R.; Liu, H.; Botton, G. A.; Baranova, E. A. Electrochemical Valorization of Glycerol on Ni-rich Bimetallic NiPd Nanoparticles: Insight into Product Selectivity Using In-situ PM-IRRAS. *ACS Sustainable Chem. Eng.*, **2019**, *7*, 14425-14434.
(5) Oliveira, V.L.; Morais, C.; Servat, K.; Napporn, T.W.; Tremiliosi-Filho, G.; Kokoh, K.B. Studies of the Reaction Products Resulted from Glycerol Electrooxidation on Ni-based Materials in Alkaline Medium. *Electrochim. Acta*., **2014**, *117*, 255-262.
(6) Suzuki, N. Y.; Santiago, P. V.; Galhardo, T. S.; Carvalho, W. A.; Souza-Garcia, J.; Angelucci, C. A. Insights of Glycerol Electrooxidation on Polycrystalline Silver Electrode. *J. Electroanal. Chem.*, **2016**, *780*, 391-395.